LBL-37517
UC-401
Preprint

Lawrence Berkeley Laboratory
UNIVERSITY OF CALIFORNIA

CHEMICAL SCIENCES DIVISION

Submitted to Review of Scientific Instruments

A High-Intensity, Pulsed Supersonic Carbon Source with $C(^3P_j)$ Kinetic Energies of 0.08–0.7 eV for Crossed Beam Experiments

R.I. Kaiser and A.G. Suits

July 1995

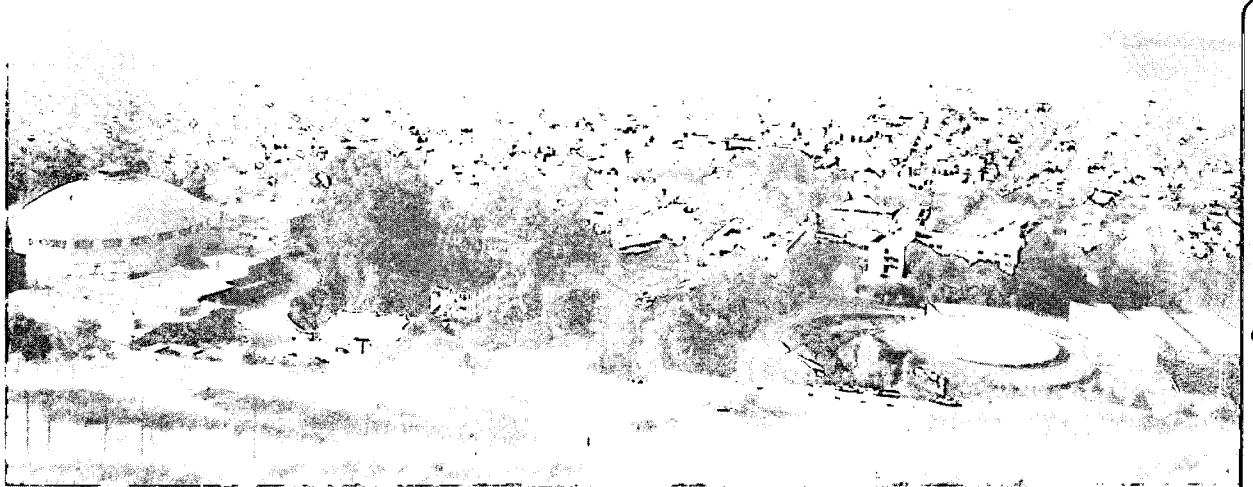

Prepared for the U.S. Department of Energy under Contract Number DE-AC03-76SF00098

DISCLAIMER

LBL-37517
UC-401

A High-Intensity, Pulsed Supersonic Carbon Source with $C(^3P_j)$ Kinetic Energies of 0.08–0.7 eV for Crossed Beam Experiments

R.I. Kaiser and A.G. Suits

Department of Chemistry
University of California, Berkeley

and

Chemical Sciences Division
Lawrence Berkeley Laboratory
University of California
Berkeley, California 94720

July 1995

This work was supported by the Director, Office of Energy Research, Office of Basic Energy Sciences, Chemical Sciences Division, of the U.S. Department of Energy under Contract No. DE-AC03-76SF00098.

A high-intensity, pulsed supersonic carbon source with $C(^3P_j)$ kinetic energies of 0.08 - 0.7 eV for crossed beam experiments

R.I. Kaiser, and A.G. Suits

Department of Chemistry, University of California and Chemical Sciences Division, Lawrence Berkeley Laboratory, Berkeley, California, 94720

A newly designed supersonic carbon-source produces carbon atoms in their $C(^3P_j)$ electronic ground states via laser ablation of graphite at 266 nm. The 30 Hz, (40±2) mJ output of a Nd-YAG laser is focused onto a rotating graphite rod with a 1000 mm focal length UV-grade fused silica plano-convex lens to an spot of (0.5±0.05) mm diameter. Ablated carbon-atoms are subsequently seeded into helium or neon carrier gas yielding intensities up to 10^{13} C-atoms cm^{-3} in the interaction region of a universal crossed beam apparatus. The greatly enhanced number density and duty cycle shift the limit of feasible crossed beam experiments down to rate constants as low as 10^{-11} - 10^{-12} cm^3s^{-1}. Carbon beam velocities between 3300 and 1100 ms^{-1}, with speed ratios ranging from 2.8 to 7.2, are continuously tunable on-line and in-situ without changing carrier gases by varying the time delay between the laser pulse, the pulsed valve and a chopper wheel located 40 mm after the laser ablation. Neither electronically excited carbon-atoms nor ions could be detected within the error limits of a quadrupole-mass spectrometric detector. Carbon clusters are restricted to ca. 10 % C_2 and C_3 in helium, minimized by multiphoton dissociation and eliminating the post-ablation nozzle region.

I. INTRODUCTION

Chemical reactions of ground state atomic carbon $C(^3P_j)$ play a major role in combustion processes [1-3], hydrocarbon syntheses [1-3], and interstellar chemistry [4-8]. Predominantly, however, energy dependent reaction cross sections, product distributions, and branching ratios are extracted from bulk experiments in flow cells and static gas cells [9-10]. This approach cannot eliminate three-body-collisions and biases a detailed picture of each reaction by stabilization of vibrationally and/or electronically excited reaction complexes or unstable intermediates. On the other hand, seeding of $C(^3P_j)$ in carrier gases generates an intense supersonic carbon beam. Performing a crossed beam experiment with the second reactant in combination with time and angular resolved product detection via a quadrupole mass spectrometer elucidates detailed information on elementary steps in chemical reactions [11-12].

Owing to the C (^3P_j) enthalpy of formation of 716.49 kJmol^{-1} [13] and its reactivity, a beam of supersonic carbon atoms is troublesome to produce. Two approaches are possible: *external* coupling of a large amount of energy into the C (^3P_j) precursor or synthesizing energetic precursors with masked carbon atoms (*internal* or *chemical* energy).

Molecules storing a huge amount of energy in their enthalpy of formation, e.g. 5-tetrazoyldiazonium chloride (1) or tetracyclo[3.2.0.0.^{2,7}0^{4,6}]-heptane-3-ylidene-tosylhydrazone lithium salt (2) widely served as carbon sources [2, 14-15]. Heating of (1) and (2) releases nitrogen, hydrogen chloride, and atomic carbon (1) or carbon and benzene (2), respectively. Actually, precursor (1) is extremely unstable: preparation is limited to 0.75 mmol and even etheric solutions are explosive at 200 K standing for less than 1 hour [14-15]. Precursor (1) undermines the purpose of molecular beam studies: carbon atoms react with benzene yielding a messy supersonic beam.

Wolf [16], Wolfgang [17], and Stöcklin [18] initiate ^{11}C- and ^{14}C-recoils by nuclear reactions, e.g. implanting protons or neutrons into gaseous nitrogen, i.e. ^{14}N (n, p) ^{14}C, and ^{14}N (p, α) ^{11}C. But as a consequence of multiple elastic/inelastic energy transfers in binary encounters of keV-recoil carbons with target molecules [19], only a broad energy distribution with $\Delta v/v >> 0.2$ (v = root mean square velocity, Δv = intensity at half maximum of velocity distribution) is achieved. In addition, the number density of recoil carbon atoms is restricted to 10^7-10^8 cm^{-3} in the source region, up to six orders of magnitude too low for feasible crossed beam applications.

Alternatively, irradiation of pyrolytic graphite at 1800 - 2500 K with keV noble-gas ions (radiation enhanced sublimation) generates predominantly atomic carbon when bombarded with 5 keV Ar^+-ions, with formation of only minor amounts of C_2 (C_1/C_2 = 25-40 at 2100 K) [20-24]. However, adaptation to molecular beams reveals the shortcomings of this method: typically, sputter yields of < 5 carbon atoms per Ar^+-ion are achieved. Assuming a maximum Ar^+-flux of 3×10^{15} $cm^{-2}s^{-1}$ of commercially available ion-guns impinging to an area of ca. 10 mm^2 and experimentally determined peak velocities of 10^3-10^4 ms^{-1}, an upper number density of $10^{11}C$ cm^{-3} in the source region is provided before supersonic expansion takes place, thus, too low to be applied in crossed beam experiments.

Another approach consists of an arc between two graphite electrodes, vaporizing graphite at 2500 - 3500 K [25]. The vapor is either seeded in a carrier gas or reacts directly with the surrounding target molecules. In spite of number densities up to 10^{18} C-atoms cm^{-3}, the production of larger carbon clusters up to C_5 as well as irreproducible electrode-surface conditions yield unstable sublimation rates and complicate this procedure.

Photolysis of carbon suboxide, C_3O_2, releases carbon atoms in their first excited ^1D (λ < 172 nm) or ground ^3P (λ < 207 nm) state [27-33]. The carbon suboxide-precursor, however, polymerizes even at 77 K, decomposes randomly during sublimation purification [34], and yields electronically excited C_2O

in the supersonic beam, interfering with reactions of carbon-atoms. Attempts have been worked out to overcome C_2O ($^3\Sigma^-$, $^1\Delta$) by two-photon dissociation, but low absorption cross sections limit the desired success.

Similarly, radiofrequency- and microwave discharges of He/CH_4-flow systems produce carbon-atoms as well as ions [3]. Unavoidable CH and CH_2-radical byproducts complicate possible applications in crossed beam techniques. Last, neutralization of accelerated carbon ions to 2 - 5000 eV by charge-exchange on tungsten wires or graphite yields carbon atoms. Space charge effects, however, limit the number density in the regime of ''chemical energies" ($E < 10$ eV) to 10^{14} C-atoms cm^{-3} in the source region [1-2].

Among the great variety of approaches, laser ablation of graphite is a promising candidate to yield a high intensity, stable and reproducible supersonic carbon source to be employed in crossed beam experiments. In 1985, Costes et al. [35-36] developed a pulsed supersonic carbon beam source based on Smalley and co-worker's laser-vaporization supersonic nozzle source [37]. Carbon atoms were generated by laser ablation of graphite at 248 nm (KrF excimer) or 266 nm (4th harmonic of a Nd-YAG. A Gentry-Giese pulsed valve operating at 10 Hz entrains laser ablated carbon atoms in the Helium carrier gas to gain supersonic carbon-atom velocities of 2140 ms^{-1} with $\Delta v/v = 0.1$-0.2. Minimization of $C_2(^1\Sigma_g^+)$ and $C_3(^1\Sigma_g^+)$ was archived by reducing the down stream channel length to 2 mm and, consequently, the downstream dwell time of ablated species to < 2 μs. Reisler et al.'s design [38-39] matches Costes' carbon source, but yields velocities between 1270 and 1790 ms^{-1} with $\Delta v/v \approx 0.2$ and 70000 ms^{-1} ($\Delta v/v = 1$; free ablation).

Both designs, however, drive the pulsed valve and laser with only 10 Hz; if shot-to-shot background subtraction is desired, the repetition rate of the Nd:YAG laser drops to 5 Hz. Additionally, number densities are limited to $< 10^{12}$ C-atoms cm^{-3} in the interaction region. Both limitations constrain

crossed beam reactions to rate constants of $k > 10^{-10}$ cm^3s^{-1}; reactions with smaller rate constants are hardly accessible with common setups. Further, current designs cannot tune the velocity of the supersonic-carbon beam continuously: this deficit, however, limits the versatility and resolution to determine energy dependent cross sections and threshold energies for endothermic reactions. The carbon pulse duration is very long and no time zero for TOF or LIF data recording is provided. Finally, quantitative distributions of carbon cluster have not been elucidated.

Therefore, the new generation of supersonic carbon sources to be constructed has to fulfill the following requirements: (a) number densities of $> 10^{12}$ C-atoms cm^{-3} in the interaction region, (b) minimizing of carbon clusters, (c) quantitative determination of ratio of carbon clusters to atomic carbon, (d) exclusion of carbon ions, (e) tunable, reproducible, and long-term stability of the supersonic carbon beam, and (f) increasing the duty cycle, (g) very short beam pulse to provide precise time origin. Finally, the life-time of $C(^1D_j)$ and $C(^1S_j)$, i.e. 53 ms and 2 s, respectively, versus typical flight times of carbon-atoms from the laser-ablation zone to the interaction region in the μs-regime enforces elimination of electronically excited carbon atoms (h).

The paper is laid out as follows: sections II.A-C describe the experimental setup, i.e. the design of the carbon source and incorporation in the vacuum system, the carbon beam generation, and data acquisition. The results focus on velocities and speed ratios of the supersonic carbon beam, beam-composition, and number-densities in the interaction region (sections III.A-C). Finally, the discussion in section IV centers on specified demands (a)-(h).

II. EXPERIMENTAL SETUP

A. Design of the carbon source

The center of the carbon source is made of a (30 mm × 40 mm × 15 mm) aluminum block, Figure 1, attached to a stainless steel frame with (50 mm × 50 mm × 300 mm) dimensions. Carbon rods, SPK purity grade with < 2 ppm ash content, are supplied by Bay Carbon Incorporation, Michigan, and were turned down to 0.53 mm outer diameter limited by the thermal expansion induced by the laser irradiation. The carbon rod is located 0.1 mm inside the extension channel of a Proch-Trickl pulsed valve with 0.75 mm i.d. nozzle [40]. The upstream channel, 1 mm i.d., extends 8 mm from the pulsed valve to the laser ablation region and intersects the 2 mm diameter laser hole channel at 90 degrees. The encountered carbon rod is interfaced to an Oriel DC motor, type 18078, and is kept in a helical motion during the laser irradiation. This design guarantees bi-directional repeatability motion with high vertical and horizontal precision over 45 mm travel length. Wobbling effects of the carbon rod are eliminated completely. A contact plate coupling the carbon rod to the motor tip triggers polarity switch of the motor via a bistable relay (Philips ECG RLY7742, 12 V DC, 15 A) after hitting a micro switch. Optionally, polarity switch can be induced by an external timer circuit. This integrated feedback system maintains a constant speed in either direction, necessary for shot-to-shot reproducibility for laser ablation of graphite. The downstream extension channel was limited to 1 mm length and opened to 6 mm inner diameter; longer channels, reduced diameters, and cone-like extensions were found to clog after 1-2 h operation hours even at low laser powers of 5 mJ per pulse. The modular design of the carbon source, i.e. the aluminum block, the stainless steel frame, and the pulsed-valve holder, allows interfacing this construction to an x-translation stage: a vacuum feedthrough manipulates the nozzle-skimmer distance and optimizes the carbon concentration at a given laser power. Additionally, moving the stainless steel frame 60 mm away from the skimmer permits changing the carbon-rod without interfering with the alignment of the source.

B. Incorporation of the carbon source in the vacuum system

The optimization of the carbon source is performed in a modified universal crossed molecular beam apparatus described in ref. [41] in detail. Briefly, the 30 Hz, (40±2) mJ per pulse, 266 nm output of a Spectra Physics GCR-270-30 Nd:YAG laser is focused on the carbon rod with a 1000 mm focal length UV-grade fused silica plano-convex lens to an spot of (0.5±0.05) mm o.d after passing a UV-grade fused silica window. This arrangement restricts the beam absorption to (4.0±0.5) %. The laser beam entrance channel is completely isolated from the second source region to avoid reaction of carbon atoms in the first source with background reactant molecules. The pulsed supersonic beam of carbon atoms (source I) and the second reactant, i.e. a continuous supersonic acetylene beam in our test experiments, (source II) pass through skimmers with apertures of 1.0 mm and 0.58 mm, attached to a differential wall to reduce the background in the reaction chamber held at typically 1×10^{-7} Torr, Figure 2, and cross at 90° with divergences of 3.0° and 4.3°, respectively. The Poch-Trickl pulsed valve operates at 60 Hz, 80 μs pulses, and 4 atm backing pressure of helium and is driven by -500 V pulses. The continuous source in region II features a 0.1 mm nozzle diameter, and a backing pressure of (563±6) Torr acetylene (Matheson, 99.5 %) purified by an acetone absorber and an acetone-dry ice cold trap. Likewise, the nozzle-interaction region distance was optimized to (61.2±0.1) mm and (27.0±0.1) mm (first source and second source, respectively).

The supersonic carbon beam or reactively scattered species were monitored using a triply differentially pumped UHV chamber, rotatable in the plane of the beams with respect to the interaction region with dimensions of (3.2 mm × 3.2 mm × 3.2 mm). Each region is evacuated by an ion pump and a magnetic suspended turbomolecular pump, yielding ca. 4×10^{-11} Torr in the third region. All turbomolecular pumps are backed by an oil-free Drytel pump. A slide valve with a 4 mm i.d. O-ring is used to

separate the reaction chamber from the first differentially pumped detector region: during on-axis operation a small detector aperture of 0.23 mm i.d. is used, whereas off-beam-axis reactive scattering experiments require a larger, 3.8 mm × 3.8 mm rectangular aperture. Differentially pumped chamber I serves to reduce the gas load from the main chamber, whereas chamber II evacuates the quadrupole mass filter, and the Daly-type scintillation particle detector [43]. Chamber III contains the Brink-type ionizer (ionization efficiency ca. 10^{-4} at 10 mA emission current [42]), surrounded by a liquid nitrogen cold shield. Two (5.8 mm × 5.8 mm) rectangles constrain the viewing angle of the ionizer nested 34.5 cm from the interaction region to 1.7° in each direction. The ionizer consists of a carbon coated thoriated tungsten filament spot welded to a gold plated stainless steel cylindrical can, a meshed wire grid, and an extractor lens held at - 800 V. The electron energy, i.e. the potential difference between the can and the grid, was optimized to 200 eV, whereas the ion energy was held at + 80 eV (potential difference between grid-potential and grounded quadrupole rod system). Extracted ions are focused by an electric lens located after the extractor plate, pass the quadrupole mass filter and are accelerated towards a stainless steel target maintained at -25 kV. The ion hits the surface and initiates an electron cascade; the electrons are accelerated by the same potential until they reach an organic scintellator whose photon cascade is detected by a photomultiplier (PMT) mounted outside the UHV detector and held between 1200 and 1700 V. The count rate is limited to 1 MHz to avoid saturation, i.e. overlapping recharge intervals of capacitors in dynode chain. Each PMT-pulse is amplified in a dual linear amplifier (LRS, model 133B) and passes a discriminator (LRS, model 621 BL) to suppress low-level noise. After converting from NIM- to TTL-standard by a level adapter (LeCroy, model 688AL), the signal is fed into two home-built multichannel scalers I (MCS I) and II (dwell time of each channel between 1 μs and 7.5 μs).

C. Carbon-beam generation and data acquisition

The time-of-flight (TOF) spectra of the supersonic carbon beam were recorded on-axis choosing the small detector aperture, c.f. section B. - A chopper wheel of 17.8 mm diameter with four 8 mm long and 1 mm wide slots located 90° apart is attached to a synchronous three-phase-motor (model 75A1004-2, Globe Motors) and spins at 240 Hz. The 960 Hz TTL output of a IR-diode (Newark Electronics, type 0PB960, configuration T) mounted at the top of the motor-supporting frame is coupled into a frequency divider (division by 16), yielding an 60 Hz external TTL trigger pulse for pulse generator I (SRS, model 535), c.f. Fig. 3. The 940 μs delayed TTL output of channel AB (pulse width = 80 μs) triggers the pulsed valve I in the primary source. In the case of reactive scattering experiments and a pulsed source II, pulsed valve II is triggered 100 μs and 102 μs - C_2H_2-reactant molecules - prior to pulsed valve I. This timing sequence limits the depletion of the carbon beam to (17.5±0.5) % and, thus, three-body collisions in the interaction region to < 3 %. A second frequency divider reduces the output of channel A to 30 Hz, triggering a) MCS I 16666.67 μs after the initial pulse, b) MCS II, and c) pulse generator II (SRS, model 535). TTL output of channel AB ignites flashlamps of the Nd:YAG-laser 16616 μs after the helium or - alternatively -16618 μs after a neon pulse (4 atm. neon backing pressure), whereas the CD-TTL output opens the Q-switch 186 μs time delayed. Raw data are accessed via a 6001 crate controller (DSPT), interfaced to a 486DX-PC. The present trigger sequence records time-of-flight-(TOF) spectra with ''laser-on'' (MCS I) and ''laser off'' to enable pulsed valve modulated background subtraction for alternate triggers (MCS II).

III. RESULTS

A. Velocity and speed ratio of the carbon beam

Figure 4 displays typical TOF-spectra of m/z=12 (C^+), 24 (C_2^+), and 36 (C_3^+), recorded with 80 eV electron energy, after optimization of experimental parameters, i.e. pulse- and delay-sequences, helium backing pressure, pulsed valve pulse-width, dimensions of the carbon source, laser power, and distance nozzle-interaction region to contribute to points a)-g), c.f. section I. The velocity of C_1, C_2, and C_3 were determined by fitting the TOFs after offset-correction, i.e. electronic offset (difference between MCS trigger-pulse and IR-diode pulse, response time of MCS I and IR diode, MCS I offset of channel AB in respect to t = 1/60 s), physical offset (misalignment of chopper wheel and IR-diode), and ion-flight time [44-45], to

(1) $$N(v) = v^2 \exp\left(-\left(\frac{v}{a} - S\right)^2\right)$$

after convolution over the ionizer length and the shutter function of the chopper wheel. The number density of molecules with velocity v, N(v), is given as a function of two additional parameters, the speed ratio S and α = m/2RT, where m is mass of the molecule (atom), T the temperature of the beam and R the ideal gas constant. This fitting routine yields supersonic velocities of the seeded carbon atoms to, e.g., $v_{(C/He)}$ = (2340±58) ms^{-1} and a speed ratio of S = (7.3±0.2), averaged over one month experimental time. Varying delay times of pulsed valve I allow a continuously tunable helium seeded carbon-beam velocity from 2100 - 3300 ms^{-1} with velocity fluctuations less than 4 %, c.f. Table I. Speed ratios increase with reduced carbon-beam velocity from 2.81±0.1 (3272±55 ms^{-1}) to 7.3±0.4 (2340±58 ms^{-1}). Higher velocities up to 3800 ms^{-1} are available, but He-Rydberg-atoms formed in the ablation interfere with measurements. The low-velocity cut-off of ca. 2100 ms^{-1} is governed by decreasing carbon beam

intensity down to ca. 10 % of the peak intensity. Lower velocities between 1800 ms^{-1} and 1100 ms^{-1}, however, are archived by varying the seeding gas to Neon (99.995 %, Matheson Gas). The excluded velocity regime of 2100 - 1800 ms^{-1} is accessible via seeding carbon atoms in He/Ne mixtures.

B. Composition of the carbon beam

The carbon beam is characterized by performing on-axis TOF-measurements between m/z = 12 (C^+), and 120 (C_{10}^+) in m/z = 12 increments at an emission current of 4 mA and an electron kinetic energy of 80 eV. Results show cluster production restricted to C_2 and C_3, if a laser power of > 10 mJ per pulse at 266 nm, i.e. > 10^{13} Wm^{-2}, is applied. Predominantly, multiphoton-dissociation destroys larger carbon clusters. The ratio of C_1: C_2:C_3 was determined by a) integrating TOF of m/z = 12 (C^+), 24 (C_2^+), and 36 (C_3^+), b) correcting for the relative ionization cross section, and c) accounting for fragmentation pattern of cations formed in the ionizer region. In the case of closed shell species without structural isomers, the ionization cross sections σ_{ion} scales with the square root of the molecular polarizability α [46] within ± 20 %:

(2) $$\sigma_{ion} = 36\sqrt{\alpha} - 18,$$

whereas the molecular polarizability is calculated as the sum of atomic-polarizabilities, i.e. yielding $\sigma_{(c1)} : \sigma_{(C2)} : \sigma_{(C3)}$ = 1 : (1.5±0.2) : (1.8±0.3). Krajnovich determined cracking patterns of the carbon clusters at 80 eV electron energy and yielded ca. 33 % fragmentation of C_3^+ to C^+ and C_2, as well as ca. 30 % fragmentation of C_2^+ to C^+ and C [47]. Correcting for this, we find relative number densities C_1: C_2:C_3 = 1 : (0.06±0.04) : (0.07±0.04) at a velocity of (2340±58) ms^{-1}. Changing from helium to neon seeding gas increases cluster-production from ca. 20 % to 70 %, c.f. Table I.

In addition, carbon- and cluster-ions were probed by a) turning the emission current of the ionizer-filament off and grounding the grid, and b) performing reactive scattering with C_2H_2 with and without an external electric field of E = 300 Vcm^{-1}; however, no C_n^+-ions could be detected. Moreover, electronically excited carbon atoms were probed in reactive scattering experiment of helium seeded carbon-atoms with molecular hydrogen: the reaction of $C(^3P_j)$ with H_2 is endothermic by 92.4 $kJmol^{-1}$ and does not produce CH-radicals sampled as CH^+ at m/z = 13:

(3) $$H_2(^1\Sigma_g^+) + C(^3P_j) \rightarrow CH(^2\Pi_j) + H(^2S_{1/2});\ \Delta_R G° = +\ 92.4\ kJmol^{-1}$$

(4) $$H_2(^1\Sigma_g^+) + C(^1D_j) \rightarrow CH(^2\Pi_j) + H(^2S_{1/2});\ \Delta_R G° = -\ 33.3\ kJmol^{-1}$$

(5) $$H_2(^1\Sigma_g^+) + C(^1S_j) \rightarrow CH(^2\Pi_j) + H(^2S_{1/2});\ \Delta_R G° = -167.4\ kJmol^{-1}$$

On the other hand, $C(^1D_j)$ and $C(^1S_j)$ yield $CH(^2\Pi_j)$. Nevertheless, not even traces of electronically excited carbon atoms could be detected. Further checks were performed by inelastic scattering of $C(^1D_j)$ with xenon-atoms with a quenching rate at 293 K $k = (1.1\pm0.3)\times10^{-10}$ cm^3s^{-1}. Likewise, no inelastic energy processes were observed and eliminate carbon in its $C(^1D_j)$ and $C(^1S_j)$ state.

C. Number density of carbon atoms in the interaction region

After a few nozzle diameters, the supersonic flow expands radially from the nozzle treated as a virtual point source [48]. In the absence of an interaction between the Mach-disc and the supersonic expansion, the on-axis (Θ = 0) number density n(R, Θ=0) at a distance R, with the nozzle diameter D and the post-nozzle distance R hold the relation

(5) $$n(R, \Theta=0) = f * n_0 * (R / D)^{-2},$$

with a scaling parameter f (f = 0.15 for monoatomic gases) and the number density in the source region n_0. The radial dependence at constant R is given by

(6) $$n(R,\Theta) = n(R,0) * \cos^2(s\,\Theta)$$

with an angular scaling parameter s (s = 1.15 for monoatomic gases). Using a known number density of helium-atoms as a calibrant at 4 atm backing pressure at 293 K, the number density of carbon atoms in the interaction region can be calculated. Including the different ionization cross sections of helium and carbon of $\sigma_{(He,\ 200\ eV)} : \sigma_{(C,\ 200\ eV)} = 3.7\times10^{-17}\ cm^{-2} : 1.7\times10^{-16}\ cm^{-2}$ [49], a number density of $(0.7\pm0.3)\times 10^{13}\ cm^{-3}$, i.e. (0.3±0.1) % carbon atoms seeded in helium, in the interaction region is derived.

IV. DISCUSSION

A comparison of our operation conditions and specifications with Table II, compiling characteristics of currently operating carbon sources in crossed beam experiments, underlines the novel features of the newly designed carbon source combined with a quadrupole mass spectrometer and a chopper wheel. The continuously tunable velocity regime extends from 3300 to 1100 ms^{-1} with standard deviations of less than 5 % and, therefore, enlarges the experimentally accessible range by 1200 ms^{-1} (high velocity limit) and 200 ms^{-1} (low velocity limit), i.e. yielding collision energies in reactive scattering experiments with, e.g. acetylene (v = 866 ms^{-1}), between 8 and 48 $kJmol^{-1}$. Additionally, the increased repetition rates of the laser from 10 Hz to 30 Hz improve the duty cycle by a factor of three. Taking into consideration the higher number density of carbon atoms in the interaction region of $(0.7\pm0.3)\times10^{13}\ cm^{-3}$ versus $< 10^{12}\ cm^{-3}$ in [35-36, 38-39], reactive scattering signals increase at least by 30 fold. Therefore, the lower limit of feasible crossed beam experiments decreases to rate constants in the 10^{-11} - $10^{-12}\ cm^3s^{-1}$ domain. Seeding gases, however, should be restricted to helium and neon to avoid cluster growth at the expense of atomic carbon: helium limits cluster contribution to 10 - 25 % of C_n-species, whereas the clustering in neon expands up to 75 %.

Moreover, the new carbon source determines the composition of the carbon-beam on-line and in-situ: operation parameters were optimized by minimizing carbon clusters detectable via LIF, whereas the present setup allows beam monitoring, i.e. composition and velocity, to endure a long term-stable supersonic carbon beam. Currently, reproducible beam characteristics are accomplished ablating single carbon-rods up to 340 h. Minor drifts during the experiments and intensity fluctuations are compensated by varying the delay-time of the pulsed valve and the laser, i.e. picking a different part of the gas pulse, and adjusting the focus of the 1000 mm lens onto the rotating carbon rod. Further, characterization of the carbon beam depicts a complete absence of electronically excited carbon atoms and ions.

Summarized, the present, modular design of the carbon source will gain an enormous boost in the reaction dynamics of carbon atoms as well as other refractory elements via crossed-beam experiments. Threshold energies for endothermic reactions, e.g., can be simply elucidated by tuning the carbon-beam velocity. Future projects are aimed to extend the energy regime by increasing the wheel frequency to 400 Hz, reducing the slot-width from 1 mm to 0.1 mm and performing a free ablation: only a 0.4 μs window of a free-ablation-carbon-pulse is transmitted. Preliminary experiments limit the velocity regime to ≈ 8.5 eV.

ACKNOWLEDGMENTS

One of us, R.I.K., is indebted the Deutsche Forschungsgemeinschaft for a post-doctoral fellowship. Both of us would like to thank Prof. H. Reisler, USC, for valuable discussion regarding the carbon-source. This work was supported by the Director, Office of Energy Research, Office of Basic Energy Sciences, Chemical Sciences Division of the U.S. Department of Energy under Contract No. DE-AC03-76SF00098.

REFERENCES

[1] Reactive Intermediates in the Gas Phase, D.W. Setser, ed., Academic, New York (1979).

[2] Reactive Intermediates, R.A. Abramovich, ed., Plenum, New York (1980).

[3] Short-Lived Molecules, M.J. Almond, ed., Ellis Horwood, New York (1990).

[4] K. Roessler, H.J. Jung, B. Nebeling, Adv. Space Res., 4, 83 (1984).

[5] K. Roessler , Rad. Eff. 99, 21 (1986).

[6] R.I. Kaiser, R.M. Mahfouz, K. Roessler, Nucl. Instr. Meth. B 65, 447 (1992).

[7] E. Herbst, H.H. Lee, D.A. Howe, T.J. Millar, Mon. Not. Roy. Astrono. Soc. 268, 335 (1994).

[8] T.J. Millar, E. Herbst, Astron. Astrophys. 288, 561 (1994).

[9] A.J. Dean, D.F. Davison, R.K. Hanson, J. Phys. Chem. 95, 183-191 (1991).

[10] W. Braun, A.M. Bass, D.D. Davis, J.D. Simmons, Proc. Roy. Soc. A 312, 417-434 (1969).

[11] G. Scoles, Atomic and Molecular Beam Methods, Volume 1, Oxford University Press, New York (1988).

[12] Y.T. Lee in reference [11], p. 553.

[13] Handbook of Chemistry and Physics, D.R. Lide, ed., CRS, BocaRaton (1993).

[14] P.B. Shevlin, J. Am. Chem. Soc. 94, 1379 (1972)

[15] M.L. McKee, G.C. Paul, P.B. Shevlin, J. Am. Chem. Soc. 112 3374(1990).

[16] A.P. Wolf, Adv. Phys. Org. Chem. 2, 201(1964).

[17] R. Wolfgang, Prog. React. Kinet. 3, 97, (1965).

[18] G. Stöcklin, Chemie heißer Atome, VCH, Weinheim (1969).

[19] W. Eckstein, Computer Simulation of Ion-Solid Interaction, Springer, Berlin (1991).

[20] V. Philipps, K. Flaskamp, E. Vietzke, J. Nucl. Mat. 111/112, 781 (1982).

[21] E. Vietzke, V. Philipps, K. Flaskamp, J. Winter, S. Veprek, J. Nucl. Mat. 176/177, 481 (1990).

[22] V. Philipps, E. Vietzke, R.P. Schorn, H. Trinkaus, J. Nucl. Mat. 157, 319 (1988).

[23] V. Philipps, E. Vietzke, H. Trinkaus, J. Nucl. Mat. 179-181, 25 (1991).

[24] E. Vietzke, K. Flaskamp, M. Hennes, V. Philipps, Nucl. Instr. Meth. B 2, 617 (1984).

[25] P.S. Skell, J.S. Havel, M.J. McGlinchey, Acc. Chem. Res. 6, 97 (1973).

[26] D. Husain, L.J. Kirsch, Chem. Phys. Let. 8, 543 (1971).

[27] D. Husain, L.J. Kirsch, Chem. Phys. Let. 9, 412 (1971).

[28] D. Husain, L.J. Kirsch, J. Photochem. 2, 297 (1973/74).

[29] D. Husain, D.P. Newton, J. Chem. Soc. Farad. Trans. 78, 51 (1982).

[30] D. Husain, A.N. Young, J. Chem. Soc. Farad. Trans. 71, 525 (1975).

[31] W. Braun, A.M. Bass, D.D. Davis, J.D. Simmons, Proc. Roy. Soc. 312, 417 (1969).

[32] C.E.M. Strauss, S.H. Kable, G.K. Chawla, P.L. Houston, I.R. Burak, J. Chem. Phys. 94, 1837 (1991).

[33] D.C. Scott, J. de Juan, D. Schwartz-Lavi, H. Reisler, J. Phys. Chem. 96, 2509 (1992).

[34] H. Reisler, University of California, Los Angeles, private communication (1994).

[35] G. Dorthe, M. Costes, C. Naulin, J. Joussot-Dubien, C. Vaucamps, G. Nouchi, J. Chem. Phys. 83, 3171 (1985).

[36] M. Costes, C. Naulin, G. Dorthe, G. Daleau, J. Joussot-Dubien, C. Lalaude, M. Vinckert, A. Destor, C. Vaucamps, G. Nouchi, J. Phys. E 22 1017 (1989).

[37] D.E. Powers, S.G. Hansen, M.E. Geusic, A.C. Pulu, J.B. Hopkins, T.G. Dietz, M.A. Duncan, P.R.R. Langrindge-Smith, R.E. Smalley, J. Phys. Chem. 86, 2556 (1982).

[38] S.A. Reid, F. Winterbottom, D.C. Scott, J. de Huan, H. Reisler, Chem. Phys. Let. 198, 430 (1992).

[39] H. Reisler in Abstract for the 17th combustion research contractors meeting, Wisconsin (1995)

[40] D. Proch, T. Trickl, Rev. Sci. Instr. 60, 713 (1989).

[41] Y.T. Lee, J.D.McDonald, P.R.LeBreton, D.R. Herschbach,, Rev. Sci. Instr 40, 1402 (1969).

[42] G.O. Brink, Rev. Sci. Instr. 37, 857 (1966).

[43] N.R. Daly, Rev. Sci. Instr. 31, 264 (1960).

[44] M.S. Weis, Ph.D. thesis, University of California, Berkeley (1986).

[45] M. Vernon, LBL-Report 12422 (1981).

[46] R.E. Center, A. Mandl, J. Chem. Phys. 57, 4104 (1972).

[47] D.J. Krajnovich, Alamaden Research Center, private communication (1995).

[48] P.C. Engelking, Chem. Rev. 91, 399 (1991).

[49] K.L.Bell, K.B. Gilbody, F.J. Smith, J. Phys. Chem. Ref. Data 12, 891 (1983).

Table I. Typical characteristics of the carbon beam in crossed beam experiments.

set	seeding gas	velocity, ms^{-1}	speed ratio	C1 : C2 : C3
1	He	3272 ± 55	2.81 ± 0.1	$1 : (0.04 \pm 0.02) : (0.2 \pm 0.1)$
2	He	2518 ± 10	4.65 ± 0.1	$1 : (0.1 \pm 0.05) : (0.25 \pm 0.05)$
3	He	2340 ± 58	7.3 ± 0.4	$1 : (0.06 \pm 0.04) : (0.07 \pm 0.04)$
4	Ne	1177 ± 3	6.4 ± 0.05	$1 : (0.7 \pm 0.1) : (2.5 \pm 0.3)$

Table II. Characteristics of currently operating carbon sources in crossed beam experiments.

wavelength, nm	length & diameter upstream channel, mm	length & diameter downstream channel, mm	pulse energy, mJ	downstream dwell time, µs [3]	gas volume per pulse, mm^3	% C	FWHM, gas pulse, µs	repetition rate pulsed valve & laser, Hz	$C_1:C_2:C_3$	helium backing pressure, atm	velocity, ms^{-1}	Δv/v	reference
248	8, 1	8 [1], 1	10	2	8	< 0.9 [2]	10	10, 10	not determined	10	2140	0.1-0.2	35-36
266	8, 1	8 [1], 1	25	2	8	< 2.3 [2]	10	10, 10	not determined	10	2140	0.1-0.2	35-36
266	?	?	3.5	?	40	< 1.1 [2]	50 -	10, 10 -, 10	not determined	7.5 -	1270-1790 70000	0.2 [4] 1 [5]	33-34
266	8, 1	-	38±2	-	36	0.7±0.3	80	60, 30	1: (0.06±0.04): (0.07±0.04)	4	3300-1100	< 0.15	present work

[1] last 6 mm: 90° cone

[2] estimated

[3] the pumping speed S through nozzle with nozzle diameter d is given by $S = p * (d / 2)^2 * v$ with the velocity of a gas with molecular mass m at temperature T in the pulsed valve extension channel $v = \sqrt{\gamma RT / m}$, whereas γ is defined as the ratio of specific heats at constant pressure and volume, respectively, i.e. $\gamma = c_{mp}/c_{mV}$. The residence time t of ablated carbon atoms in downstream extension nozzle with volume V is calculated by t = V/S.

[4] seeded ablation

[5] free ablation

Fig. 1. Schematic top (a) and three-dimensional view (b) of the aluminum block of the carbon-source.

Fig. 2. Schematic top view of the crossed molecular beam setup: DET, detector; IR, interaction region; S1, source 1; S2, source 2; PV, pulsed valve; L, laser; M, motor; CW, chopper wheel.

Fig. 3. Pulse-sequence in the crossed-beam experiments. Optionally, the pulsed valve can be replaced by a continuous source.

Fig. 4. Time-of-flight-spectra of m/z=12 (C^+), 24 (C_2^+), and 36 (C_3^+), recorded with 80 eV electron energy. (a) parameter set 3, Table I; (b) parameter set 4, Table II.

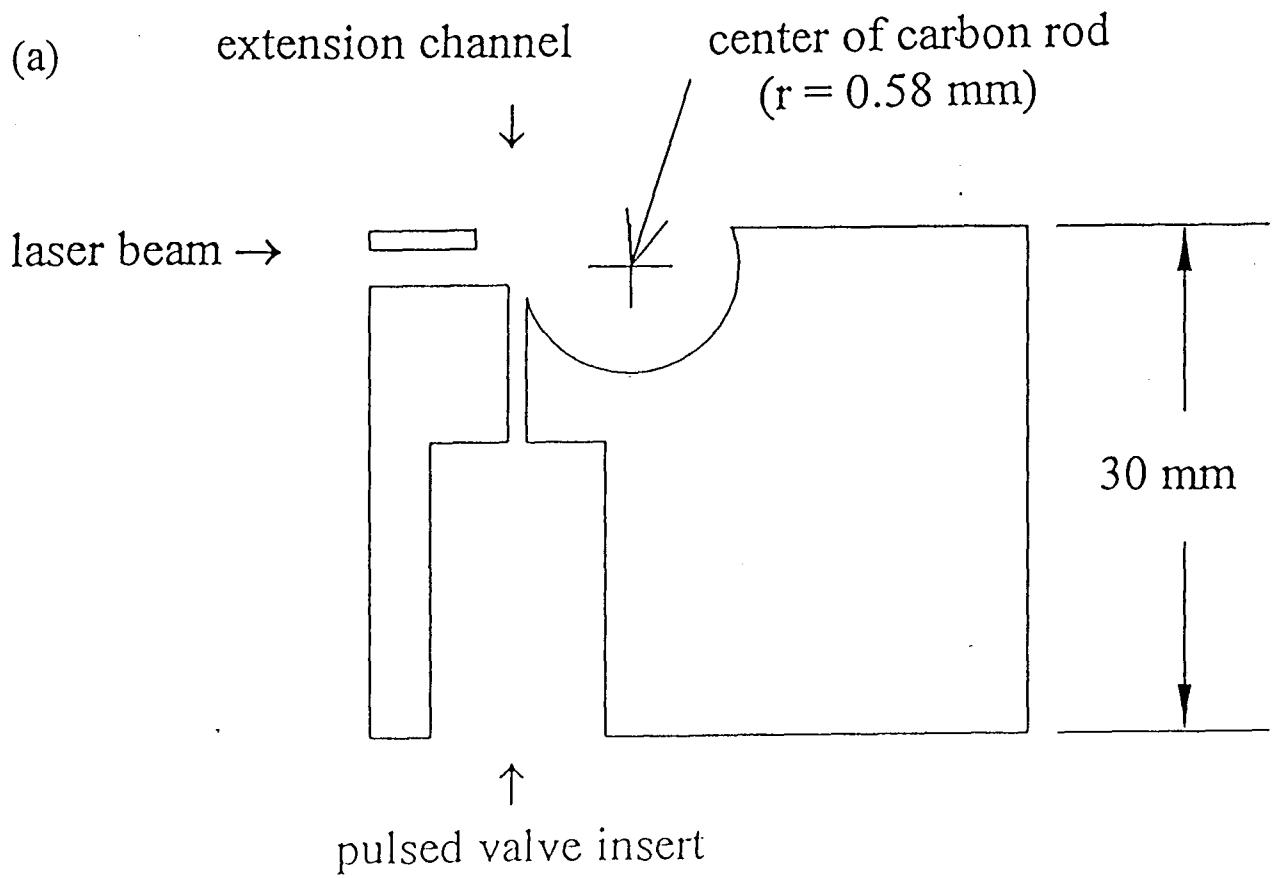
(a)
extension channel
center of carbon rod
(r = 0.58 mm)
laser beam →
30 mm
pulsed valve insert

(b)

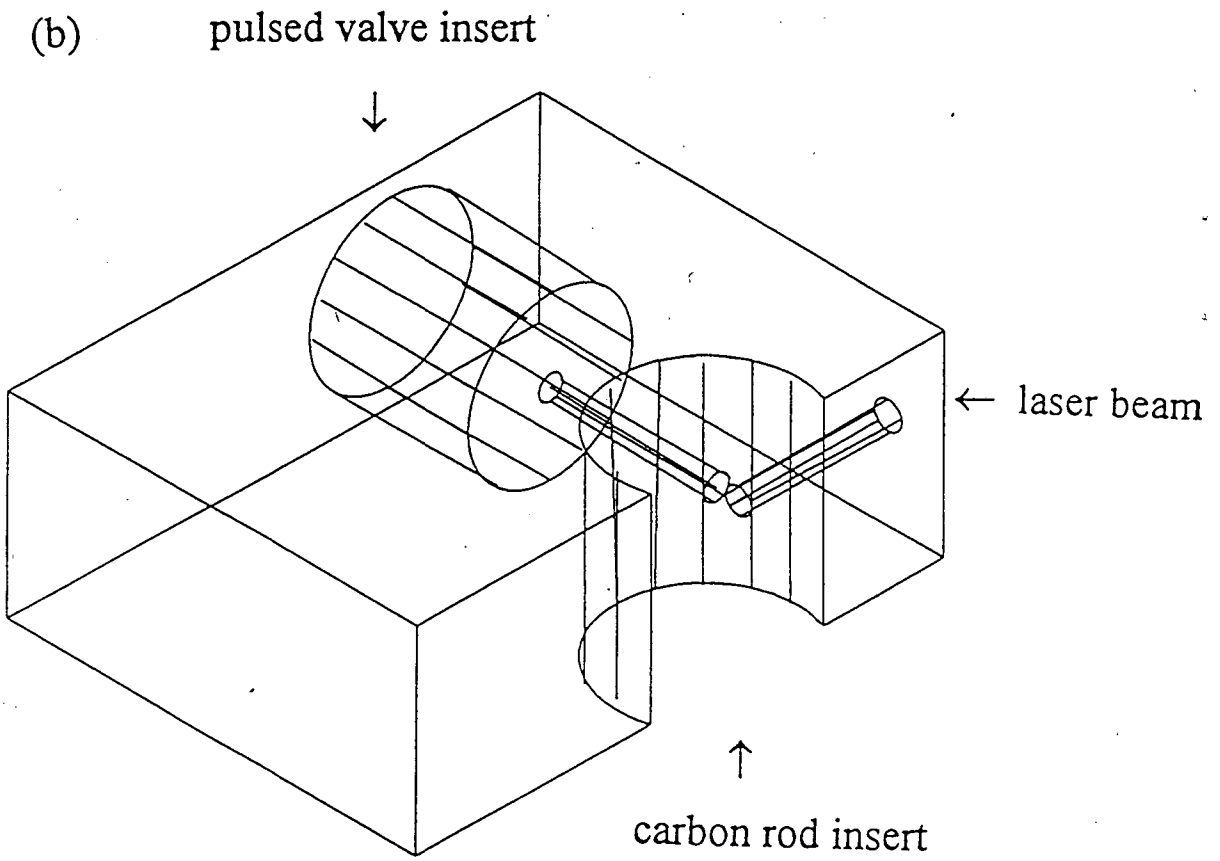

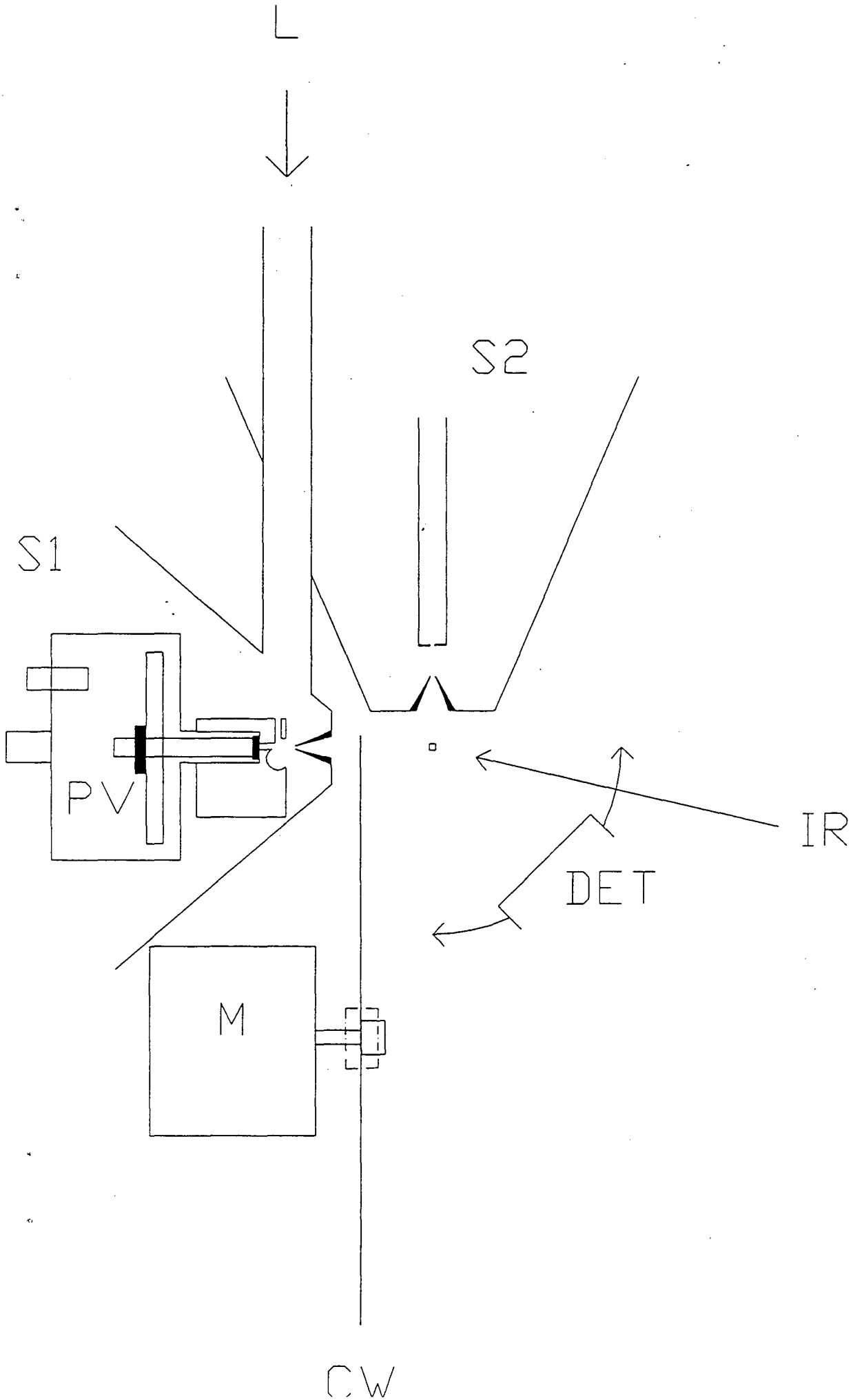
L
S2
S1
PV
IR
DET
M
CW

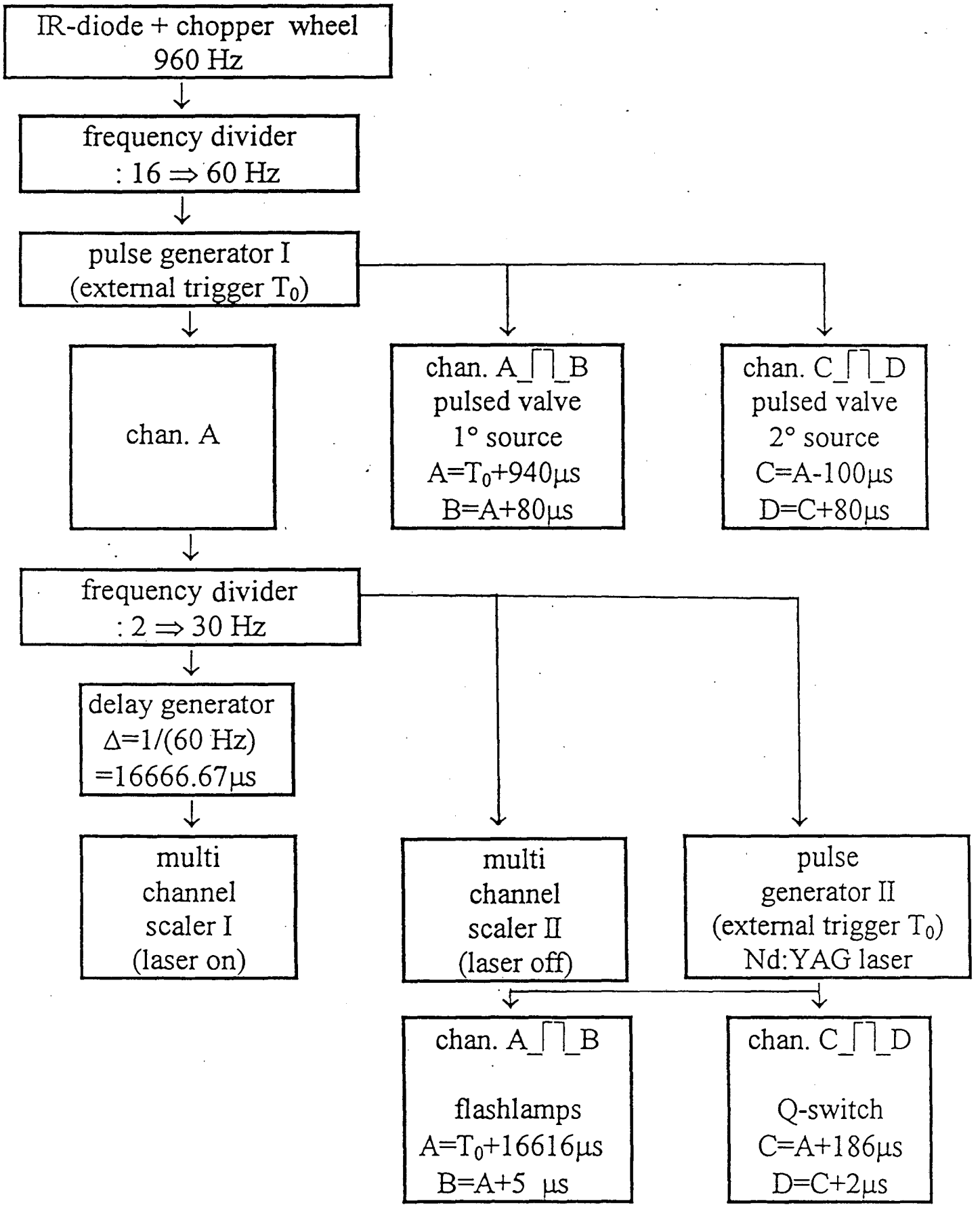
IR-diode + chopper wheel
960 Hz
frequency divider
: 16 ⇒ 60 Hz
pulse generator I
(external trigger T_0)
chan. A
chan. A_⎍_B
pulsed valve
1° source
A=T_0+940µs
B=A+80µs
chan. C_⎍_D
pulsed valve
2° source
C=A-100µs
D=C+80µs
frequency divider
: 2 ⇒ 30 Hz
delay generator
Δ=1/(60 Hz)
=16666.67µs
multi
channel
scaler I
(laser on)
multi
channel
scaler II
(laser off)
pulse
generator II
(external trigger T_0)
Nd:YAG laser
chan. A_⎍_B
flashlamps
A=T_0+16616µs
B=A+5 µs
chan. C_⎍_D
Q-switch
C=A+186µs
D=C+2µs

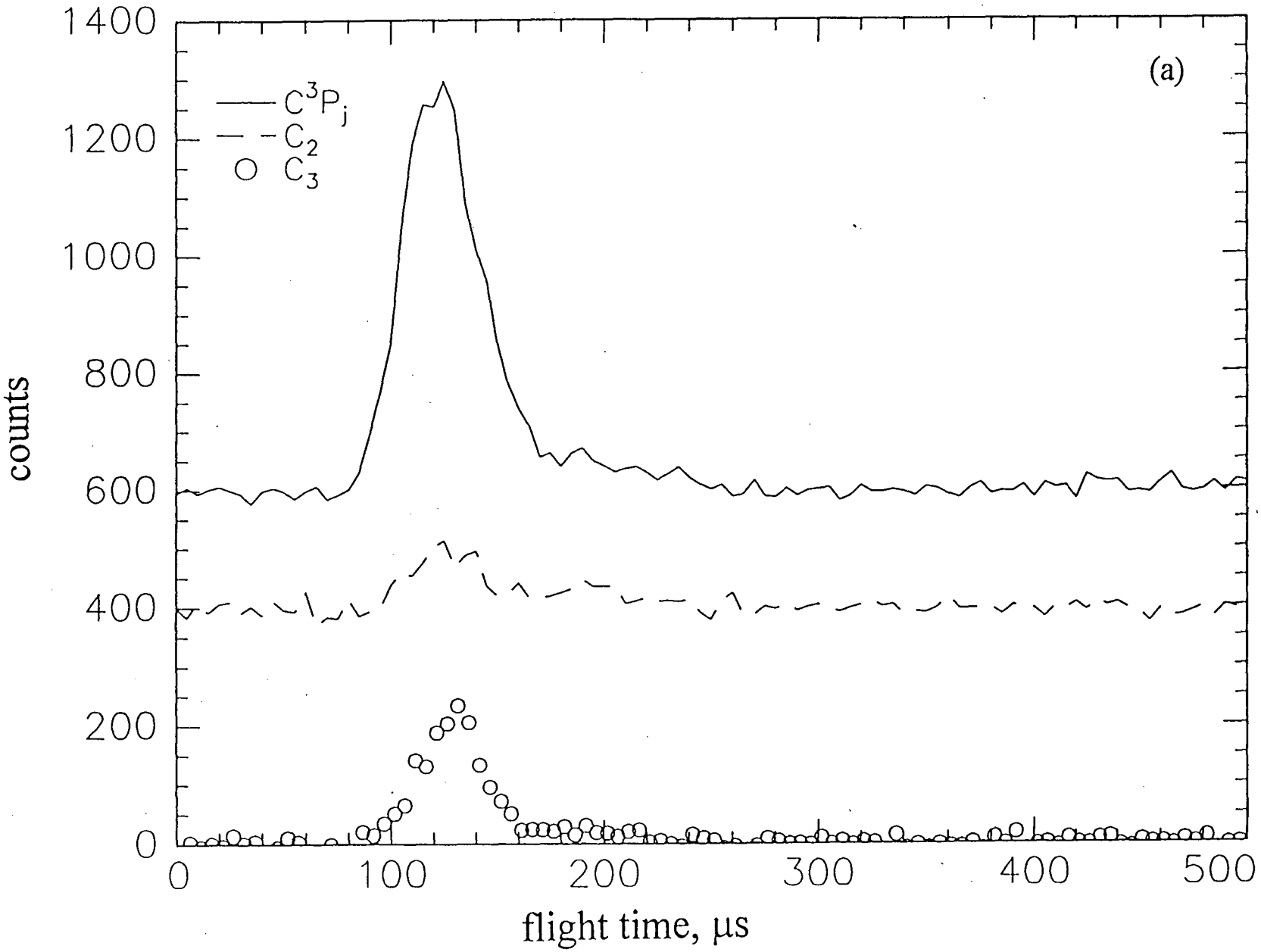
(a)
C^3P_j
C_2
C_3
counts
flight time, μs
0
200
400
600
800
1000
1200
1400
0
100
200
300
400
500

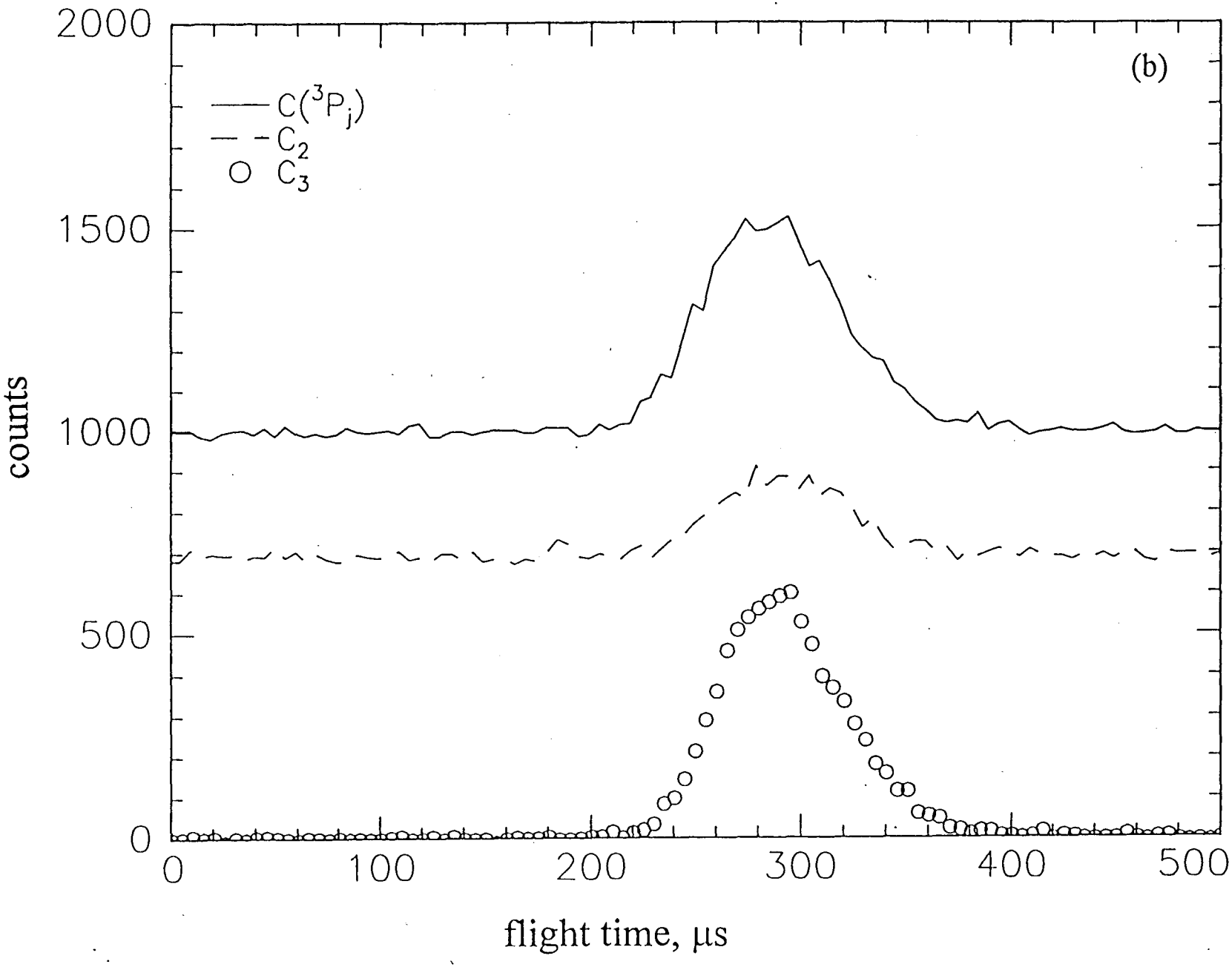
(b)
C(3Pj)
C2
C3
counts
2000
1500
1000
500
0
0
100
200
300
400
500
flight time, μs

LAWRENCE BERKELEY LABORATORY
UNIVERSITY OF CALIFORNIA
TECHNICAL INFORMATION DEPARTMENT
BERKELEY, CALIFORNIA 94720